Characterization of the Internal Structure of Landmines Using Ground-Penetrating Radar

Federico Lombardi, *Member, IEEE*, Hugh D. Griffiths, *Fellow, IEEE*, Maurizio Lualdi, and Alessio Balleri

Abstract—One of the principal limitations of employing a ground-penetrating radar (GPR) for landmine detection is the presence of clutter, i.e., reflections from the surrounding environment, which might interfere with the landmine echoes. Clutter presents similar scattering characteristics as typical targets and may significantly raise the detection threshold of the system. The capability to characterize the internal structure of a buried target might provide key unique information to develop advanced landmine–clutter discrimination algorithms, considering that the presence of internal scattering components can be univocally associated with man-made targets. In this letter, the possibility of identifying and characterizing these contributions from the GPR signature of a landmine is numerically assessed and experimentally validated. The simulated response from a landmine-like target shows that the presence of an internal structure generates additional reflection peaks, as a consequence of the layered structure of the object, and the field trials corroborate that it is possible to identify these scattering components and delineate their spatial distribution.

Index Terms—Ground-penetrating radar (GPR), landmine imaging, radar image reconstruction, trace positioning.

I. Introduction

ALTHOUGH, in recent years, significant progress has been made on ground-penetrating radar (GPR) for landmine detection [1], discriminating landmines from natural clutter remains a critical challenge [2], due to the wide possibility of clutter sources and soil temporal and spatial variability [3]. In this framework, understanding the electromagnetic signature of landmines and identifying the scattering features [4] that can uniquely define the nature of the target and unambiguously characterize a landmine can provide a step-change in the discrimination performance [5].

A common characteristic of cased man-made objects, including landmines, is the presence of a number of internal components that allow the device to function. A landmine, for example, can be modeled as a composite dielectric cylinder with a number of layers, which when illuminated produce

multiple reflections that can interfere in providing the overall target signature and radar cross section (RCS) [6].

The vast majority of clutter targets are not hollow, and therefore the detection of internal scattering components in the target radar signature can be unambiguously associated with a composite object. Consequently, a system's capability to detect the internal target components might lead to the development of advanced classification algorithms and ultimately offer improved landmine–clutter discrimination performance [7].

In this letter, numerical simulations have been carried out to characterize the electromagnetic response of a modeled landmine-like target to investigate and demonstrate the effects of the internal structure on the GPR signature. Experimental results from a field trial are then presented that validate the simulations and prove that the internal components could indeed be detected and properly characterized. The foreseen innovation is given by the fact that the investigated features are characteristic of the target itself and are not only source-independent but also scenario-independent, although the strength of radar return may vary.

This letter is organized as follows: Section II presents the results of a numerical analysis to give theoretical evidence for variations in the target radar signature produced by the presence of internal assemblies and to validate the research scope, while in Section III, the results of an experimental campaign are presented and discussed. Finally, conclusions are presented in Section IV.

II. Landmine Radar Signature Characterization

The possibility of properly identifying the reflections associated with internal structure scattering in the landmine radar signature depends mainly on: 1) the target scattering characteristics, as targets with different geometrical and/or physical properties will have a different RCS and 2) the GPR-range resolution, being the limit of certainty in distinguishing between two close scatterers.

To assess the impact of these two parameters, a number of numerical simulations have been carried out employing gprMax, an open-source finite-difference time domain (FDTD) solver available at http://www.gprmax.com [8].

The modeled environment consisted of a homogeneous sandy material hosting a target buried at a depth of 10 cm, value that recalls the requirement of the clearance programs [9]. The source was a theoretical Hertzian dipole fed with a Ricker waveform

$$s(t) = \left(1 - 2\pi^2 f_0^2 \cdot t^2\right) \exp\left(-\pi^2 f_0^2 t^2\right) \qquad (1)$$

This article has been accepted for inclusion in a future issue of this journal. Content is final as presented, with the exception of pagination.

2   IEEE GEOSCIENCE AND REMOTE SENSING LETTERS

TABLE I
NUMERICAL MODEL PARAMETERS

Parameter	Value
Domain size	50 x 80 cm
Spatial discretisation (dx, dy)	$0.1 - 0.05$ cm
Time window	12 ns
Time discretization	0.0015 ns
Number of cells	$8 \cdot 10^5$
Antenna separation	6 cm
Antenna height	1 cm
Central frequency	1.7 GHz
Frequency span	2 GHz
Soil dielectric (ε_{soil})	4.5
Target depth	10 cm
Target height	6.5 cm
Target width	8 cm
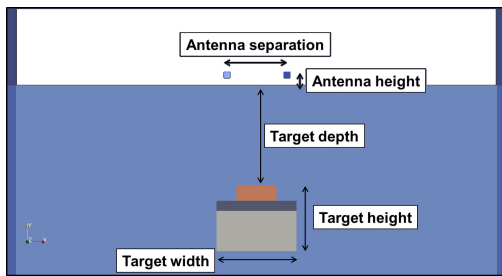
Fig. 1. gprMax modeled scenario and parameter indication.

TABLE II
INTERNAL LAYER CHARACTERISTICS

Layer	Velocity	Temporal extension
Activator pad	11.3 cm/ns	0.13 ns
Air layer	30 cm/ns	0.03 s
Main body	17.3 cm/ns	0.24 ns

Fig. 2. MATLAB-simulated signal analysis. (a) Activator pad. (b) Air layer. (c) Main body.

Fig. 3. Landmine-like object simulated response. (a) Activator pad. (b) Air layer.
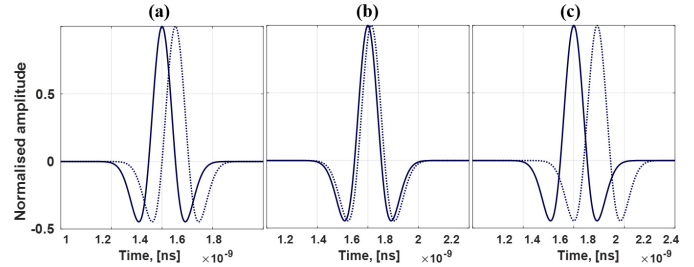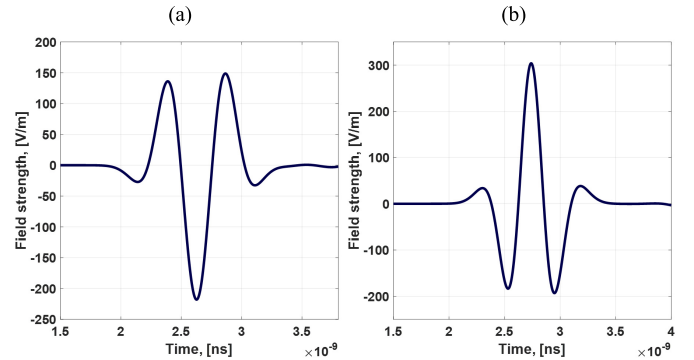
with a central frequency (f_0) of 1.7 GHz and an approximate frequency band of 2 GHz [10].

The model parameters are detailed in Table I and Fig. 1.

The landmine-like object has been modeled, which is composed of the following:

1) An activator pad (orange area in Fig. 1), characterized by a relative dielectric constant (ε_{pad}) of 7 and a thickness of 1.5 cm.
2) An air layer ($\varepsilon_{air} = 1$), representing the internal structure (dark gray area in Fig. 1) with a thickness of 1 cm.
3) The main body of the mine (light gray area in Fig. 1), characterized by a relative dielectric constant (ε_{expl}) of 3 and a thickness of 4 cm.

From this simplified sketch, the radar signature is expected to produce three different contributions, even if the possibility of distinguishing each of them is to be verified.

As a general rule, two events can be distinguished if the targets are separated in time by a time difference at least equal to the −3-dB envelope width. The considered waveform exhibits a −3-dB envelope width of approximately 0.22 ns, resulting in a required time difference between the top and the bottom of each layer of 0.22 ns in order to be separated. To evaluate the expected discrimination performance, Table II specifies the temporal extension, given the material properties of the previously described internal layers.

From the table, it is inferable that the main body is the only contribution that could be correctly reconstructed, as the time separation between the top and the bottom of the layer is sufficiently wide. For the other two components, none of them are likely to be correctly reconstructed.

These considerations are described in Fig. 2, showing the computed analytical signal and the corresponding envelope together with the delayed version according to the temporal extension of each layer.

For a system with a flat-frequency response, the pulsewidth equals the reciprocal of the bandwidth, and the required bandwidth for the activator pad to be resolved is on the order of 4 GHz, while for the air layer, due to its high velocity of propagation and the reduced thickness, this value almost quadrupled. For most of the currently employed GPR systems, the tradeoff between penetration and resolution has been solved by choosing a central frequency in the range 1–3 GHz, from which it follows that under realistic operating conditions, only a partial target reconstruction can be achieved.

Despite being theoretically independent from the surrounding soil characteristics, the ground additionally acts as a low-pass filter, placing a window across the antenna aperture, and thus limiting the effective dominant wavelength of the signal.

Proceeding with the analysis of the target signature, Fig. 3 shows the gprMax-simulated signatures of the activator pad and the air layer.

In accordance with the previous hypothesis, the contribution from the activator pad [Fig. 3(a)] is described by a single reflection event, also exhibiting a reverse in polarity due to
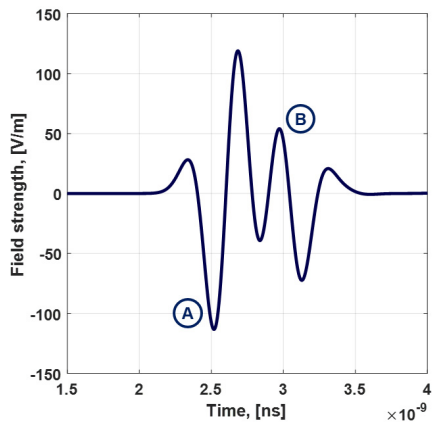
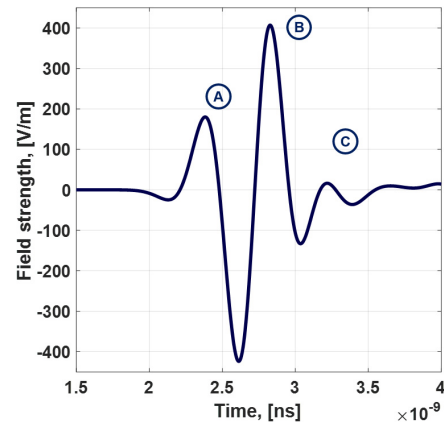Fig. 4. Landmine-like object simulated response: main body component.

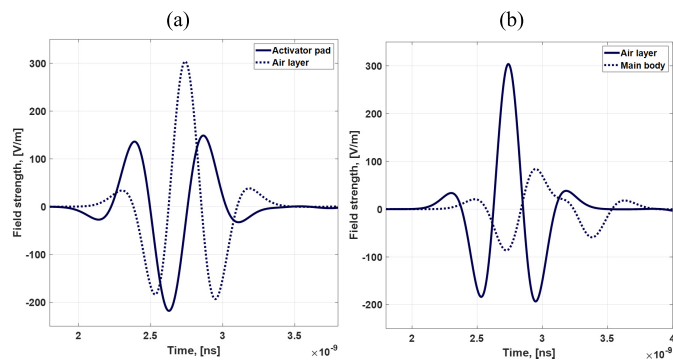Fig. 6. Simulated response from a landmine-like target.

Fig. 5. Landmine-like object simulated temporal occurrence analysis. (a) Activator pad and air layer component. (b) Air layer and main body component.

Fig. 7. Comparison between a landmine-like target and a homogeneous one.

a change in the reflection coefficient sign ($\varepsilon_{pad} > \varepsilon_{soil}$). The same behavior, except for the polarity reversal, can be highlighted for the air layer contribution [Fig. 3(b)], similarly characterized by a regular scattering function.

The response from the main body, as shown in Fig. 4, exhibits two closely spaced events (marked A and B), belonging to the top and the bottom of the layer, both exhibiting reversed polarity. In this case, the vertical extension of the layer is higher than the resolution limit and the layer can be properly reconstructed. In particular, the peak-to-peak two-way travel time is approximately 0.45 ns, in agreement with the value in Table II, resulting in a computed layer thickness close to the specified one (4 cm).

Finally, the effects of the mutual interference of the three layers due to their temporal succession needs to be addressed and, as in the previous analysis, the three contributions have been considered as separate events. Fig. 5 shows the temporal occurrence of the reflection events according to the internal geometry of the target.

From Fig. 5(a), the interference between the reflections is expected to result in two well distinguishable peaks, given the location of the two signature components. On the contrary, the width of the air layer contribution [Fig. 5(b)] is likely to completely merge with the one generated by the main body, possibly limiting its detectability.

These considerations are confirmed when analyzing the overall signature of the landmine-like target, shown in Fig. 6.
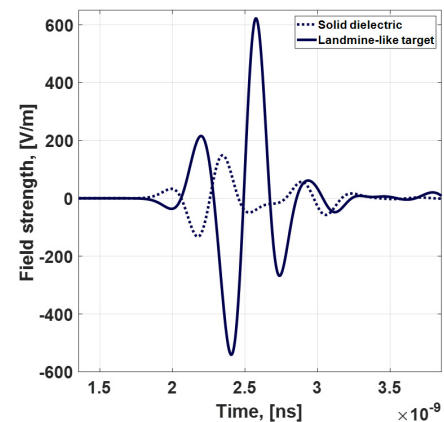
Consistent with Fig. 5, the three components lose their individual identity, and hence prevent a straightforward reconstruction and interpretation of the result. However, the hypothesis of a heterogeneous target rather than a solid one can be supported by the fact that the signature is visibly asymmetric, both analyzing the time separation of the peaks and their relative amplitudes. In particular, it is possible to safely identify three events: the top and bottom reflections (respectively, marked A and C in Fig. 6), and a sharp reflection (marked B in Fig. 6) occurring between these two, which can be associated with the scattering contribution produced by the internal air layer.

Therefore, a blind reconstruction of the target would lead to estimating the object as a composition of at least two different layers, the latter one characterized by high dielectric contrast and high velocity. A hint on the presence of a third layer can be made considering the peak-to-peak amplitude difference in the late reflections (marked B and C in Fig. 6), which might imply a reflection overlap and the polarity outline of the latter one (marked C in Fig. 6).

As a final analysis, the comparison of the landmine-like target signature with the one generated by a solid homogeneous dielectric one, with the same dimensions and characterized by a dielectric constant (ε_{solid}) of 3, is provided in Fig. 7.

The time separation of the top and the bottom of the homogeneous target (approximately 0.37 ns) is sufficient for the target to be reconstructed, and consequently its signature exhibits two reflections, spaced 0.36 ns and a stable behavior

This article has been accepted for inclusion in a future issue of this journal. Content is final as presented, with the exception of pagination.

4

IEEE GEOSCIENCE AND REMOTE SENSING LETTERS

Fig. 8. Neutralized landmine. (a) External view. (b) Disassembled target [11].

TABLE III
FIELD ACQUISITION PARAMETERS

Parameter	Value
Acquired area	50 x 50 cm
Spatial sampling (dx, dy)	0.4 − 0.8 cm
Time window	20 ns
Time sampling	0.0522 ns
Antenna separation	6 cm
Antenna height	< 1 cm
Antenna frequency	2 GHz
Antenna bandwidth	2 GHz
Soil dielectric (ε_{soil})	4.5
Target depth	10 cm
Target height	3.5 cm
Target width	8.8 cm

between them. What can be additionally noticed is that the landmine-like target signature has a longer extension, in agreement with the presence of a faster medium.

In conclusion, it can be said that despite being partially under the resolution performance of the system, the object can be correctly identified as a composite target.

III. EXPERIMENTAL VALIDATION

The numerical analysis has been validated through a 3-D field survey, employing a representative inert landmine model (pictured in Fig. 8), complete with all of its parts and filled with a highly explosive simulant.

The target was buried with the activator pad facing the surface at a depth of approximately 10 cm, in a sandy material characterized by a relative dielectric constant (ε_{soil}) of roughly 4.5. The GPR equipment employed for the measurements consisted of an IDS Aladdin radar (provided by IDS Georadar srl), an impulse device carrying dipole antennas separated by 6 cm with a central frequency and a bandwidth of 2 GHz.

Details of the field experimentation are provided in Table III.

Except for time calibration, performed through an autocorrelation function, and a frequency filtering to remove the out-of-band noise, no additional processing steps have been applied on the data.

The acquired GPR signature of the target is presented in Fig. 9.

Three separate events can be identified, with a close correlation with the numerical results previously obtained and commented: the upper part of the landmine, a sharp reflection
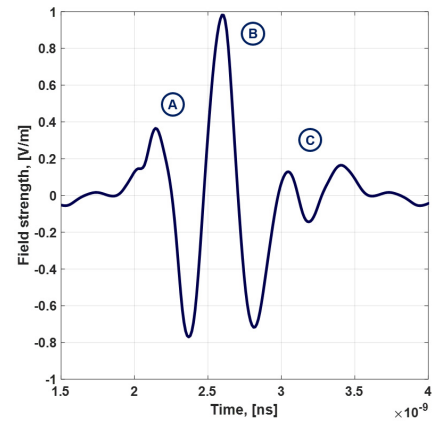

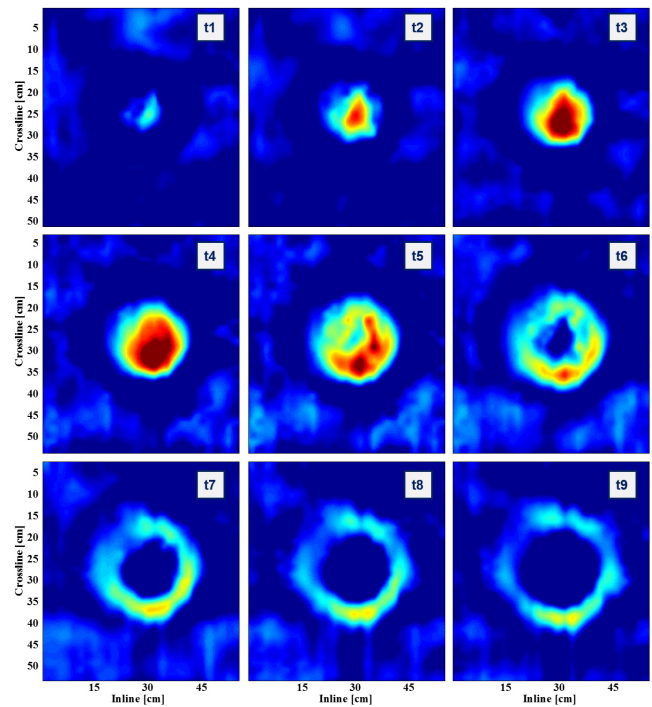Fig. 9. Experimental response from a landmine-like target.

Fig. 10. SB-33 radar time slice. Order from left to right, top to bottom.

after it, and a weak response indicating the bottom of the target (respectively, marked A–C in Fig. 9), exhibiting a slightly more complex pattern probably due to the internal design of the target. Therefore, the internal structure contribution has confirmed to provide a reliable feature for identifying the target.

The results of the 3-D analysis are presented in Fig. 10 and shown in terms of a set of time slices, i.e., the horizontal sections of the volume taken at a specified time instant. The GPR slices are displayed in a blue–yellow–red colourmap and with normalized amplitude values.

The results demonstrate the capability of GPR to delineate the internal structure reflections' spatial distribution, thus providing enhanced information on the target.

In particular, the slice at $t4$ shows a uniform high reflectivity area centered in the middle of the target, indicating a regular scattering element smaller than the target and located at
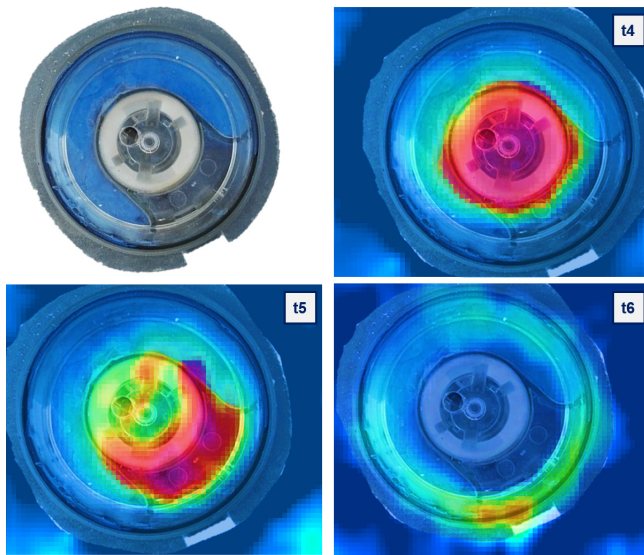
Fig. 11. Optical overlay of the radar results with the actual device.

its center. The hint on the contour of the feature arises from the fact that the maxima of the reflections are concentrated in a single location, with the amplitudes gradually decreasing following a hyperbolic behavior. In the following slice ($t5$), the reflection distribution identifies a semicircular shape, possibly generated by a number of scattering events near the outer border of the target. Also, in this case, the extended element supposition, rather than a single-point scatterer, comes from the analysis of the amplitude peaks' pattern. The target contribution in the subsequent slices ($t6$ onward) is reduced due to the effect of the highly reflective layer.

In conclusion, the internal structure of the target can be considered consisting of a regular central element and a high scattering region covering only a part of it.

The imaging performance can be better evaluated by overlaying the radar results with the landmine cutaway, as provided in Fig. 11, in which the correspondence between the actual design and the supposed structure is plainly visible.

The central scattering feature highlighted in the radar slice $t4$ is confirmed to be the fuse and striker assembly, which has a regular cylindrical shape. The radar anomaly marked $t5$, instead, appears compatible with the void area of the landmine, positioned beside the fuse and encompassing it, both in terms of location and shape. This also validates the absence of data in the successive slices.

Finally, the overlay also provides a further correspondence for the circular evidence ($t6$): superimposing the two images, one can note that the bolder part represents the detonator capsule signature.

IV. CONCLUSION

The possibility for characterizing the internal structure of a buried target from its radar images might represent a significant achievement for increasing the performance and efficiency of GPR for landmine detection.

The outcomes of the research have demonstrated that, despite the limited thickness of its assemblies, which means that only a partial reconstruction is achievable due to

resolution limits, the internal structure of a landmine does have a noticeable effect on the target signature, in both ideal and more realistic conditions.

In addition, the GPR slices showed that the internal structure can be geometrically delineated and reconstructed with a very close correspondence with the actual physical structure.

Ongoing developments are focused on determining the robustness of the approach, both in terms of GPR system configuration and target characteristics reliance. First of all, the experiment and the simulations were all carried out considering proximal operations, i.e., a limited antenna–ground surface separation, to maximize the energy coupling process, and consequently the target scattering contribution. Progressively elevating the source from the ground is expected to alter the pattern of the landmine signature and potentially lead to a reduction in the detection performance. Therefore, a further investigation to quantify these effects is needed, considering also the potential advantage of operating the system at a stand-off distance. Other key parameters that are currently researched are the impact on the landmine structure detectability of a change in the target inclination angle and its burial depth.

REFERENCES

[1] D. J. Daniels, "An assessment of the fundamental performance of GPR against buried landmines," *Proc. SPIE*, vol. 6653, May 2007, Art. no. 65530G, doi: 10.1117/12.715142.

[2] A. Genc and G. B. Akar, "Combination of physics-based and image-based features for landmine identification in ground penetrating radar data," *J. Appl. Remote Sens.*, vol. 13, no. 2, p. 1, Apr. 2019, doi: 10.1117/1.JRS.13.026503.

[3] X. Núñez-Nieto, M. Solla, P. Gómez-Pérez, and H. Lorenzo, "GPR signal characterization for automated landmine and UXO detection based on machine learning techniques," *Remote Sens.*, vol. 6, no. 10, pp. 9729–9748, Oct. 2014.

[4] C. R. Ratto, P. A. Torrione, and L. M. Collins, "Exploiting ground-penetrating radar phenomenology in a context-dependent framework for landmine detection and discrimination," *IEEE Trans. Geosci. Remote Sens.*, vol. 49, no. 5, pp. 1689–1700, May 2011, doi: 10.1109/TGRS.2010.2084093.

[5] O. Lopera, N. Milisavljevic, D. Daniels, and B. Macq, "Time-frequency domain signature analysis of GPR data for landmine identification," in *Proc. 4th Int. Workshop, Adv. Ground Penetrating Radar*, Aula Magna Partenope, Italy, Jun. 2007, pp. 159–162, doi: 10.1109/AGPR.2007.386544.

[6] F. Lombardi, H. D. Griffiths, L. Wright, and A. Balleri, "Dependence of landmine radar signature on aspect angle," *IET Radar, Sonar Navigat.*, vol. 11, no. 6, pp. 892–902, Jun. 2017, doi: 10.1049/iet-rsn.2016.0491.

[7] F. Lombardi, H. D. Griffiths, and A. Balleri, "Landmine internal structure detection from ground penetrating radar images," in *Proc. IEEE Radar Conf.*, Oklahoma City, OK, USA, Apr. 2018, pp. 1201–1206, doi: 10.1109/RADAR.2018.8378733.

[8] C. Warren, A. Giannopoulos, and I. Giannakis, "GprMax: Open source software to simulate electromagnetic wave propagation for ground penetrating radar," *Comput. Phys. Comm.*, vol. 209, pp. 163–170, Dec. 2016, doi: 10.1016/j.cpc.2016.08.020.

[9] *International Standards for Humanitarian Mine Clearance Operations*. Accessed: Jan. 22, 2020. [Online]. Available: http://www.un:org/Depts/mine/Standard/glossary:htm

[10] Y. Wang, "Frequencies of the Ricker wavelet," *Geophysics*, vol. 80, no. 2, pp. A31–A37, 2015, doi: 10.1190/GEO2014-0441.1.

[11] D. Ressler, "Study of the effects of aging on landmines," CISR Studies and Reports, James Madison Univ., Harrisonburg, VA, USA. Tech. Rep. 1, 2010. [Online]. Available: http://commons.lib.jmu.edu/cisr-studiesreports/1